Kinetic synergistic transitions in the Ostwald ripening processes

I N Sachkov, V F Turygina and A N Dolganov

Ural Federal University named after the first President of Russia B.N.Yeltsin, Yekaterinburg, Russia

e-mail: v.f.volodina@urfu.ru

Abstract. There is proposed approach to mathematical description of the kinetic transitions in Ostwald ripening processes of volatile substance in nonuniformly heated porous materials. It is based upon the finite element method. There are implemented computer software. The main feature of the software is to calculate evaporation and condensation fluxes on the walls of a nonuniformly heated cylindrical capillary. Kinetic transitions are detected for three modes of volatile substances migration which are different by condensation zones location. There are controlling dimensionless parameters of the kinetic transition which are revealed during research. There is phase diagram of the Ostwald ripening process modes realization.

1. Introduction

Thermal Ostwald ripening process is one of the essential mechanisms of substance migration. The process consists of the fact that material located in the hot zone of temperature heterogeneous systems evaporates, and its vapors migrate and then condense on cooler surfaces. The effect of the Ostwald ripening on layer formation was found in technologies such as microelectronics [7], laser radiation effect [8], protoplanetary cloud material formation [9], nuclear power objects [10], etc.

However, several features of process associated with diffusion interaction of evaporation and precipitation zones remained outside the field of view of researchers. Heretofore, there are no approaches that allow to predict the kinetic synergistic transitions of Ostwald ripening process in non-uniformly heated capillary-porous medium.

2. Task setting

A non-uniformly heated cylindrical cavity is considered as an element of the capillary-porous medium. A volatile matter is placed on the hot base of the cavity. This matter vaporizes and diffuses into the volume of the cavity and in background gas medium. Then the vapor condenses on the cooler areas of cavity surface.

The cavity radius is equal to R_0 and its length – L_0. Using a cylindrical coordinate system (R,Y) the origin of coordinates is aligned with the center of more heated cylinder base. The Y axis is directed along the cavity axis. In this case we proceed to dimensionless variables in equations (1), (2), (3) shown in figure 1. Limitations in the present section are given by studying the features of the processes which have changing gas and cavity surface temperature, T, monotonically changes along Y from T_e (evaporating end) to T_{con} (condensing end) and does not depend on the radius.

$$r = \frac{R}{L_0} \quad (1)$$

$$y = \frac{Y}{L_0} \quad (2)$$

$$r_0 = \frac{R_0}{L_0} \tag{3}$$

3. Theory

The features of Ostwald ripening are being researched which realized in a cylindrical cavity with a quadratic temperature changing law along the Y axis as in equation (4).

$$\theta(y) = \theta_{ey} - \Delta\theta(1 - A_2)y + A_2 y^2 \tag{4}$$

where A_2 – quadratic rate parameter ($-1 \le A_2 \le 1$).

Three ways of vapor diffusion are expected and shown in figure 1. γ is a condensation only on the cold end of the cavity, α – precipitation on the base and on the whole side surface of the cylinder, β – at the end and part of the side surface. Let us determine the conditions under which the discussed modes α, β and γ are realized. We establish distribution of precipitation and condensation fluxes on the cavity surface.

For the purpose it is necessary to calculate concentration field of the volatile component (its partial pressure) P (r, y). The solution of the problem is possible by using the finite element method. Previously, the method shows great flexibility in describing processes of transport and phase transformation realized in spatially heterogeneous systems [1-5]. Algorithms is the basis of developed computer software presented in excellent book referenced by [6].

Taking the variation approach, according to which the diffusion equation is equivalent to extreme functionality condition as in equation (5), [1-6].

$$X = \int_{V_c} D\ (grad\ P)^2\ d\ V \tag{5}$$

where V_c – cylindrical cavity volume, D – diffusion rate of volatile component vapors in background gas medium as in equation (6)

$$\mathrm{D} = \mathrm{D_O} \times \mathrm{T}^{3/2} \tag{6}$$

D_0 – practically independent of temperature constant.

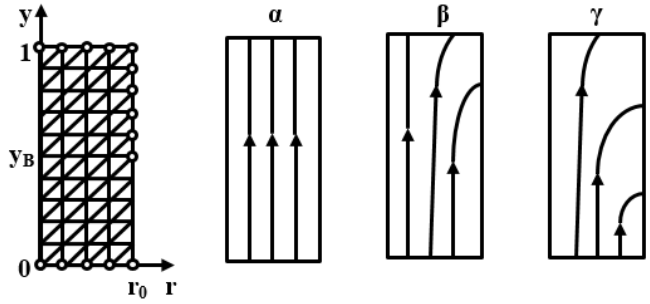

Figure 1. Dividing workspace on simplex-elements schemes and diffusion lines of Ostwald ripening modes patterns α, β and γ. White circles – boundary conditions implementing of the first type; y_B – condensation and clean surface areas boundary.

The finite element method [1-6] is used to find the field function P(r, y) that minimizes the function in equation (5). The area of two-dimensional space is sampled by triangular simplex elements. The uniform grid divides volume cross-section into triangular elements in figure 1. The pressure is approximated by a linear function within each triangular element as in equation (7).

$$P^e = \alpha^e\ r + \beta^e\ y + \gamma^e \tag{7}$$

The volume differential stated in equation (8) helps to take into account the problem spherical symmetry.

$$\mathrm{dV} = 2\pi \mathrm{r^e}\ \mathrm{dr}\ \mathrm{dy} \tag{8}$$

where r^e – radius of gravity center of triangle "e". Thus, the contribution of each element out of "e" volume to the functional X is defined by equation (9).

$$X^e = 2\pi\, r^e\, D^e \int_{Se} (\text{grad}\, P^e)^2\, dr\, dy \quad (9)$$

Here S^e – square of the triangular element, $D^e = D(r^e, y^e)$ – diffusion coefficient calculated at the center area of "e"-element temperature.

There are three types of inner surfaces: evaporating, condensing and free from migrating matter. The boundary conditions are established for them. The boundary conditions of the first type are established for nodes which are located on evaporating and condensing end (i.e. at y = 0 and y = 1 respectively) and also on the side surface at $r = r_0$ and $0 < y < y_B$ (where condensing process takes place – white circles in figure 1). It means that nodal values P_j are equal to saturated vapor pressure P_{ev}. The polyterma P_{ev} (T) are described by Clapeyron's equation (10).

$$P_{ev} = B_o \exp(-1/\theta) \quad (10)$$

$$\theta = \frac{R_g T}{Q_{ev}} \quad (11)$$

where θ – dimensionless temperature, Q_{ev} – evaporation heat, R_g – gas constant, T – local surface temperature.

Functional extremum conditions of equation (5) lead to a system of linear algebraic equations for the set of nodal pressure values $\{P^i\}$. The procedure of its solution described pretty well by the reference [6].

As a result, continuous distribution P(r,y) is replaced by the piecewise linear relationship. The values of fluxes density, especially precipitation and evaporation, determined by value $D\ grad\ P^e$.

There is a problem in using of the approach. The problem is to find condensing area boundary and "clean" surface on the side surface of cylinder under condition of adiabatic process. An iterative process is used to find the value of y_B. It is important that the amount of density of condensing flux is a continuous function of coordinates and goes to zero at $y = y_B$. The start value of boundary must be defined as well. Next step is to calculate the pressure P (R, Y) and the flux density D (P/R) at the point of surface with coordinate y_B. If the flux value is not equal to zero, the value y_B will be changed by a certain amount (for example, by 5%) and estimated at new boundary point. Further, new approximate value y_B is calculated using two coordinates values, their respective fluxes and pruner's method. The iterative process continues until the flux density is equal to zero on the boundary (or becomes less than defined value). It is necessary to transform partition grid on each step of process to increase accuracy of calculations by the following way: one of grid lines passed through the boundary node at y_B coordinate.

The above statements become the basis of computer software which allows to investigate profiles of condensing and evaporation fluxes on the ends and the side surface of the cavity, to gain the information about irregularity of thickness of formed layers and about mass flow ratio condensing on the side surface and the cold end. Source code is written in the Fortran language.

4. Results of computer experiments

Calculations of concentration fields and flux density of condensation and evaporation on the inner surfaces of the cavity are performed at the varying values θ_{ev}, θ_{con}, A_2 and r_0. The calculation results show that they greatly depend on the relative cavity radius r_0 and temperature parameters Δθ and θ_{ev} as in equation (12). If the control dimensionless parameter is the same the results are slightly different.

$$\Delta\theta = \theta_{ev} - \theta_{con} \quad (12)$$

where Δθ – relative maximal temperature differential.

The calculation results are summarized in the form of a chart in figure 2. It represents stability conditions of the three modes of the Ostwald ripening.

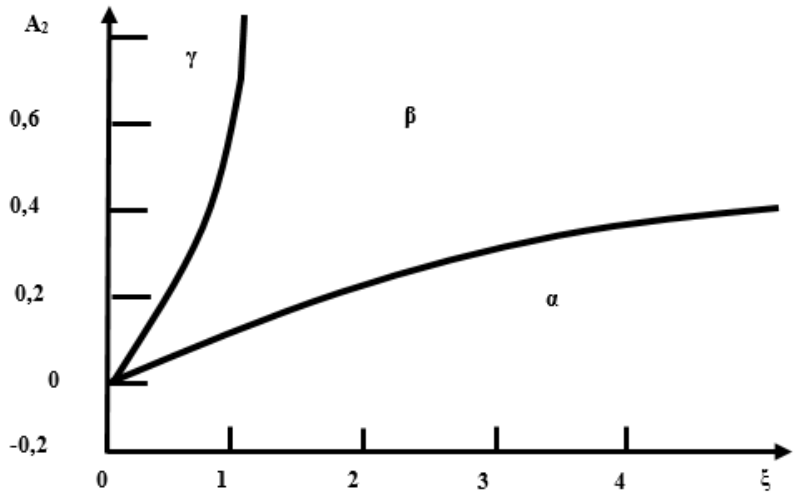

Figure 2. Charts of stability of the Ostwald ripening modes; A_2 – temperature field quadratic parameter, ξ – dimensionless temperature differential as in equation (13), $r_0 = 0{,}1$.

$$\varepsilon = \frac{\Delta\theta}{\theta_{ev}^2} \tag{13}$$

5. Discussion of results

Analysis of result shows that the mode α is only possible if $A_2 = 0$ is strictly linear law of temperature variation along Y-axis. The condensing process takes place along the side surface of the capillary. If $A_2 > 0$ then the movement of vapors takes place along the capillary axis without condensing on its side surface at low relative temperature gradients ξ. The increase of ξ results to the formation of condensation zone on the side surface adjacent to the cooler end of the capillary. Further increase of temperature gradient makes mode α more stable. In the similar way kinetic transitions may occur as a result of variations of the parameter square of the temperature field A_2.

Thus, changes in the control parameters ξ and A_2 lead to kinetic transitions of the Ostwald ripening modes α, β and γ.

The features of their implementation are in figure 3. The representative profiles of relative deposition flux densities on the side surface of capillary are in figure 3 and in equation (14).

$$q_B = -D\frac{\partial P/\partial r}{q_0} \tag{14}$$

where D – diffusion coefficient, P – pressure of diffusing vapors, q_0 – density of evaporation flux at the center of evaporating end.

In figure 3 curves 1-4 correspond to values of dimensionless temperature differences ξ which is equal to 0.5, 1.0, 2 and 4 for curves 1-4 respectively. Square parameter is $A_2 = 0.2$.

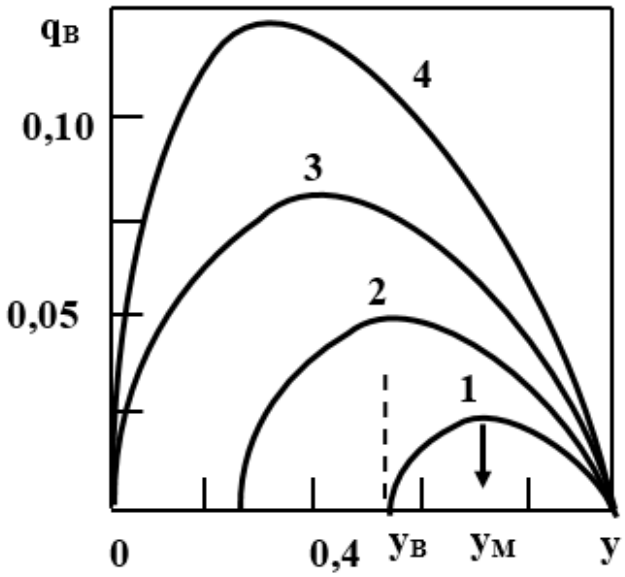

Figure 3. Transformation of profile forms of relative flux density of vapor deposition from the relative distance from the hot end depended on relative temperature difference value.

Thus, dependencies 1-2 correspond to β mode and 3-4 – to α mode. In case of small values of dimensionless temperature difference ξ there is no deposition on the side surface of the capillary – γ mode. Specific points are highlighted in the plots. Dashed line indicates position of the boundary of the condensation zone of the side surface y_B. The coordinate defines the formation of process modes. The arrow indicates axial coordinate corresponding to the maximum vapor deposition rate. Its value sets the position of the capillary section on which its occlusion is possible.

The results are illustrated by analyzing the conditions of condensing process on the side surface using simplified one-dimensional model. It is realized when the relative radius of the capillary is $r_0 \rightarrow 0$. In this case the diffusion process is grown to one-dimensional one, the vapor pressure of migrating matter linearly depends on axial coordinate as in equation (15) and the value of saturated vapor pressure is described by equation (10).

$$\frac{\partial P_{dif}}{\partial y} = -D \tag{15}$$

The ratio $P_{ev} > P_{dif}$ is the condition of condensation process. It means that the pressure of saturated vapors should be higher than the pressure provided by the diffusion.

Relationship schemes of discussed vapor pressures from the distance to the evaporating end corresponding to different process modes are stated in figure 4. In situation α the pressure of saturated vapors is higher than the pressure of diffusion and the deposition over the whole length of the capillary takes place on the side surfaces. In situation β the diffusion occurs at the beginning of the capillary and the deposition takes place on the cooler side of the capillary. In situation γ the mode of free escape of vapors from the capillary is formed.

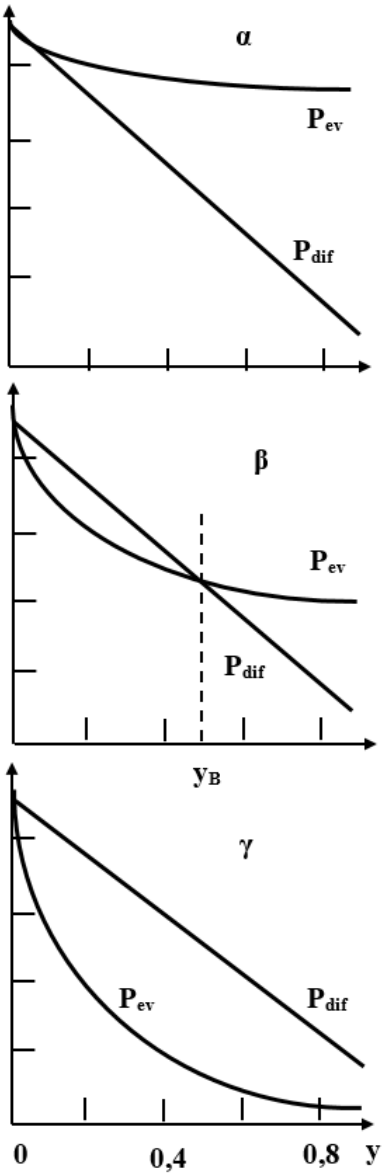

Figure 4. Dependence of vapor concentration on distance from evaporating end under conditions of free diffusion P_{dif} and saturation P_{ev}.

Thus, non-uniformly heated capillary-porous body from which evaporation of volatile matter takes place represents nonlinear dynamic system. During the growth of the temperature differential playing the role of the driving force of the process, critical phenomena occur. As the result of the flow of kinetic transitions, the picture and the intensity of vapor motion are significantly change.
Even more significant process transformations may be expected if the channel plugging capability is taken into account. The discussed phenomena are possible in α and β modes. In this case, the capillary is divided into two volumes by lengths $y_1 = y_M$ and $y_2 = (y_0 – y_M)$. It should be noted that new values of dimensionless temperature differentials ξ_1 and ξ_2 are characteristic of them. In new conditions, the processes of evaporation and condensation are started. The discussion of their laws goes beyond the scope of the present work.

6. Conclusions

The proposed approach to the mathematical description of synergistic kinetic transitions can be used to describe the processes of the migration of volatile substances in non-uniformly heated porous systems. The possibility of existence is observed in the following laws.

- It should be noted that in real porous medium there may be inclusions of different thermal conductivity. This can lead to substantial non-uniformity of the temperature field, i.e. to variations in the values ξ and A_2, and to local changes of migration mode.
- Realization of α and β modes should lead to blockage of capillaries as a result of growing of their walls. Therefore, it is possible to form extended condensation zones tied to certain points of capillary body in non-uniform porous medium.
- During the developing of α mode, it is possible for "plugs" to appear which divide the original capillary into two or more shorter ones.

Further development of research in the discussed directions is planned.

References

[1] Sachkov I N 1995 *J. High temperature* **33**:5, 759
[2] Sachkov I N 1996 *Russian J. of Phys. Chemistry* **70**:1, 111
[3] Sachkov I N and Chemerinskaya L S 2008 *Russian Phys. J.* 11(2) 165
[4] Sachkov I N, Marinova O, Turygina V F and Turygin E E 2015 The effect of the geometry of the micro pores on the effective permeability of soil (Rodos, Greece) p 4
[5] Sachkov I N, Marinova O, Turygina V F, Turygin E E and Dolganov A N 2016 Regularities of non-uniform heating of the two-phase environment during electric current *16th International Multidisciplinary Scientific GeoConference SGEM* vol 3(1) pp 599–606 DOI: 10.5593/SGEM2016/B13/S05.076
[6] Segerlind L 1984 *Applied finite element analysis* (New York: Wiley)
[7] Pavlyukevich N V, Gorelik G E and Levdansky V V 1980 *Physical kinetics and transport processes during phase transformations* (Minsk) p 208
[8] Anisimov S I, Imas Ya A, Romanov G S and Khodyko Yu V 1970 *The effect of high-power radiation on metals* (Moscow: Nauka) p 272
[9] Dorofeeva V A, Makalkin A V and Mironenko M V 1993 *Recondensation of matter in a protoplanetary disk* (Moscow: Nauka) pp 45–73
[10] Degaltsev Yu G, Ponomaryov-Stepnoy N N and Kuznetsov V F 1977 *The behavior of high-temperature fuel upon irradiation* (Moscow) p 145